Solid-State Light-Emitting Devices Based on the Trischelated Ruthenium(II) Complex. 1. Thin Film Blends with Poly(ethylene oxide)

C. H. Lyons, E. D. Abbas, J.-K. Lee, and M. F. Rubner*

Contribution from the Department of Materials Science and Engineering, Massachusetts Institute of Technology, Cambridge, Massachusetts 02139

Received March 30, 1998

Abstract: Thin-film solid-state light-emitting devices have been fabricated by using blends of a trischelated complex of ruthenium(II) with 4,7-diphenyl-1,10-phenanthroline disulfonate ligands and lithium triflate complexed poly(ethylene oxide). Charge injection occurs via an electrochemical redox mechanism and the mechanism of light production is similar to electrogenerated chemiluminescence. Orange-red light is emitted with a turn-on voltage of 2.5−3.0 V. At 6 V, devices reach luminance levels of about 100 cd/m^2 with an external quantum efficiency of 0.02% photons/electron. The admixed PEO acts both as a film processing aid, giving uniform, homogeneous, and reproducible devices, and as a polymer electrolyte for ruthenium complex and counterion diffusion. Devices reach about 50% of their maximum luminance within a few seconds, and reach maximum luminance in about a minute. This behavior can be realized without the need of elaborate charging schemes involving the use of elevated temperatures or solvent treatments that enhance ionic conductivity. Devices of this type can be fabricated via conventional processing routes and conditioned to high light ouput with a few simple voltage scans.

Introduction

The electrogenerated chemiluminescence (ECL) of both inorganic (transition metal complexes) and organic systems in liquid electrochemical cells has been studied in detail.[1−24] Of the inorganic systems, the trischelated complex of ruthenium(II) with 2,2-bipyridyl has attracted the most interest in recent years.[1−9,16−23] In this system, the excited $Ru(bpy)_3^{2+*}$ species is produced by the annihilation reaction between an electrogenerated 1+ and 3+ species as follows:[4]

$$Ru(bpy)_3^{3+} + Ru(bpy)_3^{+} \leftrightarrow Ru(bpy)_3^{2+} + Ru(bpy)_3^{2+*} \quad (1)$$

$$Ru(bpy)_3^{2+*} \rightarrow Ru(bpy)_3^{2+} + h\nu \quad (2)$$

The $Ru(bpy)_3^{3+}$ and $Ru(bpy)_3^{+}$ species can be produced alternately near the same electrode by applying a cyclic square potential wave between the reduction and oxidation potentials of $Ru(bpy)_3^{2+}$ or at opposite electrodes via the use of thin-layer DC electrochemical cells.[12] An ECL efficiency, Φ_{ECL}, of about 5% photons/electron has been reported for this system.[9] The ECL of ruthenium complexes has also been studied in aqueous solutions. In this case, it is necessary to utilize redox active additives that form reductants that can react with the oxidized Ru(II) complex such as the oxalate ion[6] or tripropylamine.[7,8]

Ruthenium complexes offer a number of very desirable features as light-emitting materials: they are chemically, electrochemically, photochemically, and thermally stable. Also, molecular engineering of the ligand system permits systematic altering of the luminescence, redox, and film forming properties of these materials. Moreover, the design criteria for tailoring these materials are well established. It has been shown, for example, that Φ_{ECL} values are strongly dependent on the nature of the ligand. The luminescence properties of many substituted derivatives of tris(bipyridyl) and tris(1,10-phenanthroline)-ruthenium(II) complexes have been investigated.[10,11,24] The highest Φ_{ECL} at room temperature (24%) has been reported for the tris(4,7-diphenyl-1,10-phenanthroline)ruthenium(II) complex in acetonitrile solution.[11] At lower temperatures, the Φ_{ECL} of this complex increases to 33%.[10]

The ECL of organic systems has also been extensively investigated. Of the organic systems, polycyclic aromatic hydrocarbons such as diphenylanthracene and rubrene have received the most attention.[13−15] Polymer-based materials have also been investigated. Recently, for example, Richter et al. have reported on the ECL of films of the conjugated polymer, 4-methoxy-(2-ethylhexoxy)-2,5-poly(phenylenevinylene) in non-aqueous solutions.[25] An ECL efficiency of about 0.4% photons/electron was obtained for this system. Pei et al. have reported

(1) Tokel, N. E.; Bard, A. J. *J. Am. Chem. Soc*. **1972**, *94*, 2862.
(2) Itoh, K.; Honda, K. *Chem. Lett*. **1979**, 99.
(3) Wallace, W. L.; Bard, A. J. *J. Phys. Chem.* **1979**, *83*, 1350.
(4) Luttmer, J. D.; Bard, A. J. *J. Phys. Chem.* **1981**, *85*, 1155.
(5) Glass, R. S.; Faulkner, L. R. *J. Phys. Chem.* **1981**, *85*, 1160.
(6) Ege, D.; Becker, W. G.; Bard, A. J. *Anal. Chem*. **1984**, *56*, 2413.
(7) Noffsinger, J. B.; Danielson, N. D. *Anal. Chem*. **1987**, *59*, 865.
(8) Leland, J. K.; Powell, M. J. *J. Electrochem. Soc*. **1990**, *1*, 257.
(9) Velasco, J. G. *J. Phys. Chem*. **1988**, *92*, 2202.
(10) Kapturkiewicz, A. *Chem. Phys. Lett.* **1995**, *236*, 389.
(11) McCord, P.; Bard, A. J. *J. Electroanal. Chem*. **1991**, *318*, 91.
(12) Laser, D.; Bard, A. J. *J. Electrochem. Soc*. **1975**, *122*, 632.
(13) Faulkner, L. R. *Int. Rev. Sci. Phys. Chem*. **1975**, *9*, 213.
(14) Faulkner, L. R.; Bard, A. J. In *Electroanalytical Chemistry;* Bard, A. J., Ed.; Dekker: New York, 1977; Vol. 10, Chapter 1.
(15) Knight, A. W.; Greenway, G. M. *Analyst* **1994**, *119*, 879 and references therein.
(16) Rubinstein, I.; Bard, A. J. *J. Am. Chem. Soc*. **1980**, *102*, 6641.
(17) Rubinstein, I.; Bard, A. J. *J. Am. Chem. Soc*. **1981**, *103*, 5007.
(18) Buttry, D. A.; Anson, F. D. *J. Am. Chem. Soc*. **1982**, *104*, 4824.
(19) Downey, T. M.; Nieman, T. A. *Anal. Chem*. **1992**, *64*, 261.
(20) Abruna, H. D.; Meyer, T. J.; Murray, R. W. *Inorg. Chem.* **1979**, *18*, 3233.
(21) Zhang, X.; Bard, A. J. *J. Phys. Chem*. **1988**, *92*, 5566.
(22) Obeng, Y. S.; Bard, A. J. *Langmuir* **1991**, *7*, 195.
(23) Xu, X.-H.; Bard, A. J. *Langmuir* **1994**, *10*, 2409.
(24) Miller, C. J.; McCord, P.; Bard, A. J. *Langmuir* **1991**, *7*, 2781.

10.1021/ja981057c CCC: $15.00
Published on Web 11/04/1998

that solid-state light-emitting electrochemical cells (LECs) based on spin cast thin films of blends of poly(1,4-phenylenevinylene) and lithium salt complexed poly(ethylene oxide)[26,27] are possible. The mechanism of light production is similar to that described by Richter et al.[25] When externally biased, the polymer layer is electrooxidized (p-type doping) at the anode and electroreduced (n-type doping) at the cathode. Electron−hole recombination occurs at a p−n type junction in the bulk of the film and light is emitted. This process is reversible. The function of the PEO is to facilitate the transport of charge compensating counterions to the oxidized and reduced sites. Luminance values of about 200 cd/m^2 at 4 V and external quantum efficiencies as high as 2% photons/electron were reported.

Solid-state light-emitting devices based on an electrochemical mechanism exhibit some interesting and desirable features. In an ideal device, (1) the turn-on voltage should equal the band gap of the electroactive emissive layer, (2) the device should operate equally well in both forward and reverse bias, and (3) the turn-on voltage should be independent of film thickness and electrode material. Hence, such devices offer a number of advantages over LED's. However, it should be noted that there are problems associated with going from a liquid state to a solid state electrochemical cell. For example, phase separation of emitter and ionically conducting components and mass transport limitations can result in slow device response times.

As noted above, most ECL studies with ruthenium complexes have been carried out in solution, where the complex is the solute or is immobilized on an electrode surface via adsorption[20−24] or a polymeric matrix.[16−19] Solid-state light-emitting devices based on thin films of these ruthenium complexes have only recently been considered. The use of these materials in display technologies clearly requires the development of high-efficiency solid-state devices. Toward this goal, Maness et al. have recently demonstrated[28,29] that solid-state electrochemically generated luminescence can be realized with ruthenium complexes via the establishment of a frozen concentration gradient of $Ru^{III/II}$ and $Ru^{II/I}$ couples. In this process, the concentration gradient is electrochemically established under conditions that favor ionic conduction and subsequently frozen-in by a cooling or drying step under a voltage bias. The net result is a faster responding light emitting system that exhibits diode-like behavior and emission efficiencies as high as 0.1%. This approach to date, however, has only produced devices with a light output that is barely detectable by the eye, most likely due to the use of interdigitated electrodes with electrode spacings that are significantly larger than those used in conventional solid-state, thin-film sandwich-type devices. Nevertheless, the very detailed work of this group has established a fundamentally important framework that can be used as the starting point for studies aimed at understanding the mechanisms of charge injection and transport in Ru(II)-based solid-state light-emitting devices. Our group, on the other hand, has recently disclosed that high brightness (our current best devices can achieve luminance levels as high as 500 cd/m^2), solid-state devices utilizing the Ru(II) complex as the emitter can be readily fabricated in the form of thin films sandwiched between suitable electrodes.[30,31] To date, our best solid-state devices exhibit external quantum efficiencies as high as 3%[31] without utilizing any elaborate pre-charging process.

This paper describes solid-state light emitting devices based on thin film blends of a trischelated complex of ruthenium(II) with 4,7-diphenyl-1,10-phenanthroline disulfonate ligands ($Ru(phen')_3^{2+}$) and poly(ethylene oxide) (PEO). Although the charge transport properties of ruthenium and osmium complexes in a PEO matrix have been extensively studied,[32−38] the application of these ruthenium complex/PEO blend systems as solid-state light-emitting devices, to our knowledge, has not been reported. The dielectric constant of amorphous PEO is about 8 at 25 °C[39] and it increases with increasing salt concentration.[40] In comparison to conventional macromolecules, this relatively high dielectric constant makes PEO a reasonably effective macromolecular solvent from the point of view of complex dissolution. In $Ru(phen')_3^{2+}$ complex devices, favorable orientation and site-to-site distances of the redox molecules are necessary for electron-transfer reactions. Hence, the microscopic-scale mobility of the redox molecules also has to be considered. The use of PEO as a solid-state electrolyte for alkali metal salts[41] and redox molecules[36−38] has been extensively studied. The solid-state electrolyte properties of PEO can therefore be exploited to improve the slow device response times associated with limited mass and ion transport.

In this paper, we will demonstrate how PEO can be used as a processing aid in thin film devices based on small molecule ruthenium complexes. Also, we will describe experiments aimed at characterizing devices based on this blend system, including how the device operates as a function of blend composition, film thickness, temperature, and electrode material.

Experimental Details

The synthesis and purification of the $Ru(phen')_3^{2+}$ complex is discussed in a previous paper.[30a] In dilute solution, this material exhibits a photoluminescence quantum yield of approximately 10%. It has the structure shown in Figure 1. PEO (M_w = 2000 g/mol) and lithium triflate salt ($LiCF_3SO_3$) were supplied by Aldrich and were used without further purification. Both the $Ru(phen')_3^{2+}$ complex and the $LiCF_3SO_3$ salt were dried under dynamic vacuum at 120 °C for 48 h prior to use. PEO was dried under dynamic vacuum at 60 °C for 48 h prior to use. All solvents were supplied by Aldrich and were used without further purification or drying. $Ru(phen')_3^{2+}$ solutions were prepared by dissolving the complex in 2-methoxyethanol to give concentrations

(25) Richter, M. M.; Fan, F.-R. F.; Klavetter, F.; Heeger, A. J.; Bard, A. J. *Chem. Phys. Lett*. **1994**, *226*, 115.
(26) Pei, Q.; Yu, G.; Zhang, C.; Yang, Y.; Heeger, A. J. *Science* **1995**, *269*, 1086.
(27) Pei, Q.; Yang, Y.; Yu, G.; Zhang, C.; Heeger, A. J. *J. Am. Chem. Soc*. **1996**, *118*, 3922.
(28) Maness, K. M.; Terrill, R. H.; Meyer, T. J.; Murray, R. W.; Wightman, R. M. *J. Am. Chem. Soc.* **1996**, *118*, 10609.
(29) Maness, K. M.; Masui, H.; Wightman, R. M.; Murray, R. W. *J. Am. Chem. Soc*. **1997**, *119*, 3987.
(30) (a) Yoo, D.; Lee, J.-K.; Handy E. S.; Rubner, M. F. *Appl. Phys. Lett.* **1996**, *69*, 1. (b) Lee, J.-K.; Yoo, D.; Rubner, M. F. *Chem. Mater*. **1997**, *9*, 1710. (c) Yoo, D.; Wu, A.; Lee, J.-K.; Rubner, M. F. *Synth. Metals* **1997**, *85* 1425.
(31) Wu, A.; Lee., J.-K.; Rubner, M. F. *Thin Solid Films*. Accepted for publication.
(32) Facci, J. S.; Schmehl, R. H.; Murray, R. W. *J. Am. Chem. Soc*. **1982**, *104*, 4960.
(33) Pickup, P. G.; Kutner, W.; Leidner, C. R.; Murray, R. W. *J. Am. Chem. Soc*. **1984**, *106*, 1991.
(34) (a) Jernigan, J. C.; Murray, R. W. *J. Phys. Chem*. **1987**, *91*, 2030. (b) Jernigan, J. C.; Murray, R. W. *J. Am. Chem. Soc*. **1987**, *109*, 1738.
(35) Dalton, E. F.; Surridge, J. C.; Jernigan, J. C.; Wilbourn, K. O.; Facci, J. S.; Murray, R. W. *Chem. Phys*. **1990**, *141*, 143.
(36) Chidsey, C. E.; Feldman, B. J.; Lundgren, C.; Murray, R. W. *Anal. Chem*. **1986**, *58*, 601.
(37) Geng, L.; Longmire, M. L.; Reed, R. A.; Parcher, J. F.; Barbour, C. J.; Murray, R. W. *Chem. Mater*. **1989**, *136*, 2565.
(38) Geng, L.; Reed, R. A.; Kim, M.-H.; Wooster, T. T.; Oliver, B. N.; Egekeze, J.; Kennedy, R. T.; Jorgenson, J. W.; Parcher, J. F.; Murray, R. W. *J. Am. Chem. Soc*. **1989**, *111*, 1614.
(39) Kaneko, M.; Wohrle, D.; Schlettwein, D.; Schmidt, V. *Makromol. Chem*. **1988**, *189*, 2419.
(40) Schlettwein, D.; Kaneko, M.; Yamada, A.; Worhle, D. *J. Phys. Chem.* **1991**, *95*, 1748.
(41) *Polymer Electrolyte Reviews*; MacCallum and Vincent, Elsevier Science: London, 1987.

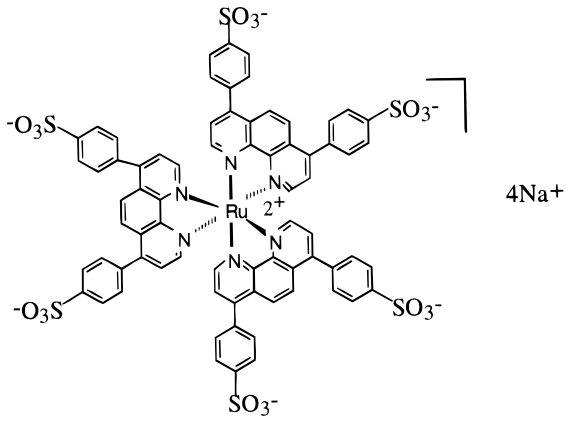

Figure 1. Structure of the trischelated complex of ruthenium(II) with 4,7-diphenyl-1,10-phenanthroline disulfonate ligands.

in the range of 4 to 5% w/v. PEO and (PEO + $LiCF_3SO_3$) solutions were prepared by dissolving the components in acetonitrile. (Ru(phen′)$_3^{2+}$ + PEO + $LiCF_3SO_3$) solutions were prepared by mixing the appropriate Ru(phen′)$_3^{2+}$ solutions and (PEO + $LiCF_3SO_3$) solutions such that the 2-methoxyethanol/acetonitrile ratio was 4:1. In those cases where the additional electrolyte was added, the molar ratio of the PEO repeat unit to $LiCF_3SO_3$ salt was 20:1. All solutions were vigorously stirred overnight and then filtered with 0.45 μm filters prior to use.

Thin film devices were fabricated by spin coating from the appropriate solution on patterned indium tin oxide (ITO) substrates with use of a Headway Photoresist Spinner. The patterned substrates consisted of four parallel lines of ITO which were 2 mm in width and 2000 Å thick. Spun cast films were further dried under dynamic vacuum at 120 °C for 2 h. Films with thicknesses in the range of 500 to 2500 Å were prepared and examined in this study. Aluminum and silver top electrodes were deposited via thermal evaporation. Platinum top electrodes were deposited by e-beam evaporation. Top electrodes were 2 mm in width and 2000 Å thick. Typically, a single ITO substrate contained 16 pixels, with each pixel having an area of 2 mm^2. Thicknesses were determined with a Sloan Dektak 8000 profilometer.

Room temperature device measurements were carried out in a drybox under a nitrogen atmosphere. Unless otherwise noted, all devices were subjected to a preconditioning procedure prior to measurements. This protocol involved repetitive cycling (typically two to three cycles) over the voltage range of interest at 100 mV/s until a stable response was observed. Current−voltage, light−voltage, current−time, and light−time characteristics were measured with a Hewlett-Packard variable voltage source with a Keithley digital multimeter and a Newport Optics silicon photodiode. Low-temperature measurements were done by attaching the sample to a liquid nitrogen coldfinger inside an evacuated Janis cryostat with the photodiode mounted to the exterior window. Temperature was regulated via a resistance heating unit mounted on the coldfinger and connected to a thermocouple feedback loop. The constant voltage-conditioned samples were preconditioned at room temperature with the same procedure as described above, allowed to stabilize at 4 V, and then cooled to the lowest temperature, generally 120 K (−153 °C), over the course of approximately 15 min while the bias was maintained. Light and current were monitored during cooling. The samples cooled without an applied bias were not preconditioned but were cooled as prepared, without ever experiencing a bias at room temperature. Forward and reverse bias data were generally obtained on different devices due to stability considerations; however, similar device performance was obtained when a single sample was used to generate both forward and reverse bias behavior.

External quantum efficiencies were calculated on the basis of the amount of light the photodiode captures from the front face of a device by using the assumption that the emission is Lambertian. According to calculations by Greenham et al.,[42] the total flux leaving a device that is not waveguided, F_{ext}, at a distance L_0 from the detector is:

$$F_{ext} = \int_0^{\pi/2} 2\pi L_0 \cos(\theta) \sin(\theta)\, d\theta = \pi L_0$$

In our case, the light collected by the photodiode, F_1, is only within the emission angles $\theta = 0$ to 21°, so we integrate only over those limits and obtain $F_1/F_{ext} = 0.1284$. We then divide our measured power output by this factor and use the corrected power, P, in the following formula:

$$\eta_{ext}(\%) = \frac{P/h\nu}{I/e}$$

where h is Planck's constant, ν is the center frequency of the emitted radiation, I is the current, and e is the elementary charge.

The maximum luminance values discussed in this paper refer to the maximum values obtainable from a device prior to device failure (usually at 5−6 V). The maximum efficiencies reported, on the other hand, were typically derived from plots of light versus current. The light versus current curves of these devices in nearly all cases were essentially linear from the onset of detection of 1 nW of light up to the maximum luminance levels (sometimes a slight rollover was observed at the highest voltages). The slopes of such curves were used to estimate device efficiency. Forward bias in this paper simply means that the ITO electrode is biased positive whereas reverse bias means the aluminum electrode is biased positive. A typical electroluminescent spectrum obtained from a thin film device based on the Ru(phen′)$_3^{2+}$ complex can be found in ref 30c.

Results and Discussion

To explore the solid-state ECL behavior of Ru(phen′)$_3^{2+}$, we first examined thin film devices comprised only of this material sandwiched between ITO and aluminum electrodes. Figure 2 shows light−voltage and current−voltage curves for a typical ITO/Ru(phen′)$_3^{2+}$/Al device. In forward bias (ITO as the anode), devices turn on uniformly at relatively low voltages, i.e., 2.5−3.0 V. Maximum luminance levels for such a device typically reach about 50 cd/m^2 with an external quantum efficiency of about 0.01% photons/electron. Currently, the best devices of this type have achieved luminance levels as high as 200 cd/m^2 at efficiencies of about 0.05% photons/electron. Also note that the current−voltage response is nearly symmetric about zero bias and does not appear to reach any limiting currents at high voltages as is frequently observed in DC operated ECL liquid devices. It can also be seen that light emission in reverse bias (Al as the anode) is negligible in these devices. The mechanism of light generation in devices of this type is likely similar to the ECL mechanism outlined in eqs 1 and 2. Hence, in forward bias, the Ru(phen′)$_3^{3+}$ species is generated at the ITO anode and the Ru(phen′)$_3^{+}$ species is generated at the Al cathode. The ion annihilation reaction between these species produces the Ru(phen′)$_3^{2+}$* excited species and light is emitted. Under DC operation, the oxidized and reduced reactants are continuously regenerated.

The film quality and device performance of the Ru(phen′)$_3^{2+}$ complex can be further improved by blending with PEO. The blend composition was optimized with respect to both film quality and device performance. Figure 3 shows how the external quantum efficiency of thin film devices varies as a function of increasing mol % of PEO repeat units. The device efficiency remains similar to that of the nonblended Ru(phen′)$_3^{2+}$ complex until PEO/Ru(phen′)$_3^{2+}$ molar ratios of about 10:1 (ca. 90 mol % PEO repeat units), after which the device efficiency starts to drop (at 99 mol % PEO (100/1 mol ratio), efficiency = 0.0064%). This is not a surprising result for a system in which electron hopping between redox centers is important. Above this composition range, it appears that the critical intermolecular distance for efficient electron hopping is ex-

(42) Greenham, N. C.; Friend, R. H.; Bradley, D. D. C. *Adv. Mater.* **1994**, *6*, 491.

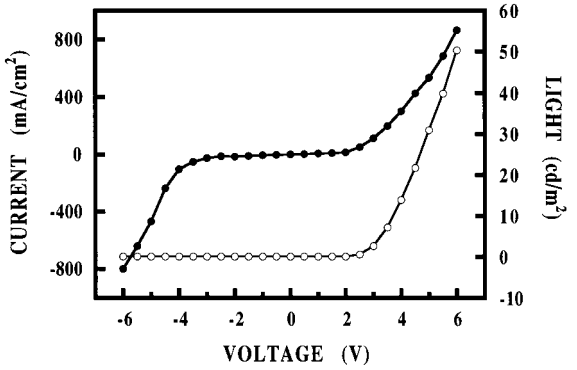

Figure 2. Light−voltage (open circles) and current−voltage (filled circles) plots for an ITO/Ru(phen′)$_3^{2+}$/Al device.

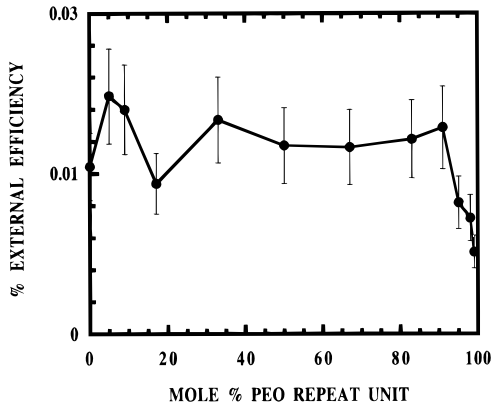

Figure 3. External quantum efficiency as a function of mol % PEO monomer unit. These values represent the maximum efficiency obtained from each system.

ceeded (there is not sufficient contact between the Ru(II) molecules and/or the Ru(II) molecules and the electrode surface to achieve efficient electron hopping).

The optimal blend composition was found to be about a 10:1 molar ratio of PEO repeat units to Ru(phen′)$_3^{2+}$ complex. Devices fabricated with this optimal composition were uniform, homogeneous, and reproducible, giving a typical external quantum efficiency of about 0.02% photons/electron. It is worth noting again that in the optimal blend compositional range, the external quantum efficiency is not much different from that of a nonblended Ru(phen′)$_3^{2+}$ device. Although the external quantum efficiency remains essentially constant at PEO/Ru(phen′)$_3^{2+}$ molar ratios less than 10:1, there are increasing problems of device nonuniformity, nonhomogeneity, and irreproducibility with devices fabricated from blend compositions with a lower PEO content.

Figure 4 shows typical light−voltage and current−voltage curves for ITO/(Ru(phen′)$_3^{2+}$ + PEO)/Al and ITO/(Ru(phen′)$_3^{2+}$ + PEO + $LiCF_3SO_3$)/Al devices under forward and reverse bias conditions. These devices were fabricated by using the optimal composition, i.e., a 10:1 molar ratio of PEO repeat unit to Ru(phen′)$_3^{2+}$. Devices were preconditioned as described in the Experimental Section. In those cases where additional electrolyte was added, the molar ratio of the PEO repeat unit to $LiCF_3SO_3$ salt was 20:1. Ionic conductivities as high as 10^{-6} S/cm have been reported for this electrolyte system (PEO + $LiCF_3SO_3$) at room temperature.[43] Comparing Figures 2 and 4, one can see that, in forward bias, these devices turn on consistently at about 2.5−3.0 V. This is close to the band gap

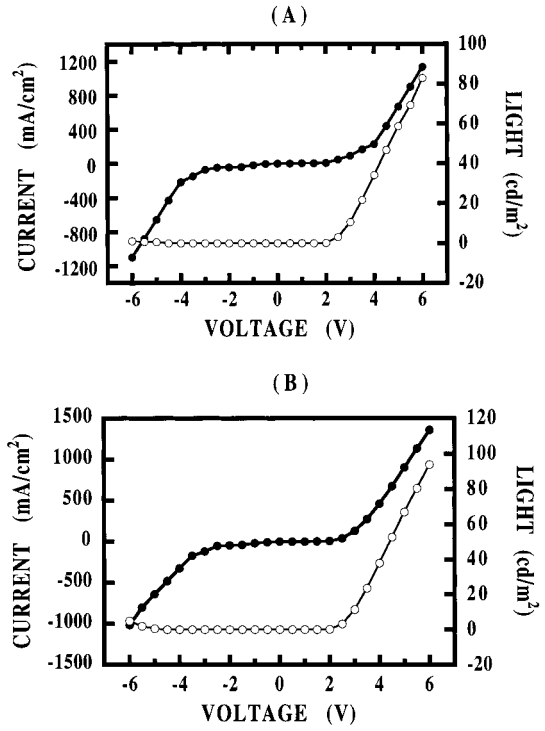

Figure 4. Light−voltage (open circles) and current−voltage (filled circles) plots for (a) an ITO/Ru(phen′)$_3^{2+}$ + PEO/Al device, and (b) an ITO/Ru(phen′)$_3^{2+}$ + PEO + $LiCF_3SO_3$/Al device.

for this material (i.e., 2.8 eV). These relatively low turn-on voltages are a desirable feature in terms of power efficiencies. In these devices, charge is injected across the electrode/emitter interface via electrochemical redox reactions. Hence, effectively, one has facile charge injection across a low resistance contact. This is in contrast to a nonelectrochemical based conjugated polymer LED device where charge injection into the resistive material occurs typically via a tunneling mechanism.[44]

Although external quantum efficiencies are similar for the three types of devices (i.e. about 0.02% photons/electron), the PEO containing devices consistently give higher luminance levels, despite the fact that the films of these devices contain a lower emitter concentration than the Ru(phen′)$_3^{2+}$ only devices. For example, maximum luminance levels for an ITO/(Ru(phen′)$_3^{2+}$/Al device are typically about 50 cd/m^2, whereas the ITO/(Ru(phen′)$_3^{2+}$ + PEO + $LiCF_3SO_3$)/Al devices can be easily pushed to maximum luminance levels of about 100 cd/m^2. This observation reflects, in part, the better film quality of the blends. Devices based just on the Ru(phen′)$_3^{2+}$ complex exhibit a much higher incidence of low voltage device failure and lower device yields and they break down more easily than the blends, particularly with thin films (500 Å). In the PEO-containing devices, one has a more uniform film with a more homogeneous distribution of the Ru(phen′)$_3^{2+}$ complex. In addition, the higher current densities possible with the blend systems (and hence higher light levels) may also reflect the enhanced nanoscopic mobility of the Ru(phen′)$_3^{2+}$ complex in the less rigid PEO matrix. Such mobility most likely involves rotational and/or translational motions of the emitter that allow for the establishment of molecular organizations more suitable for electron hopping.

Consider now the reverse bias behavior of these devices. The current−voltage response is nearly symmetric about zero bias,

(43) Walker, C. W., Jr.; Salomon, M. *J. Electrochem. Soc.* **1993**, *140*, 3409.

(44) Parker, I. D. *J. Appl. Phys.* **1994**, *75*, 1656.

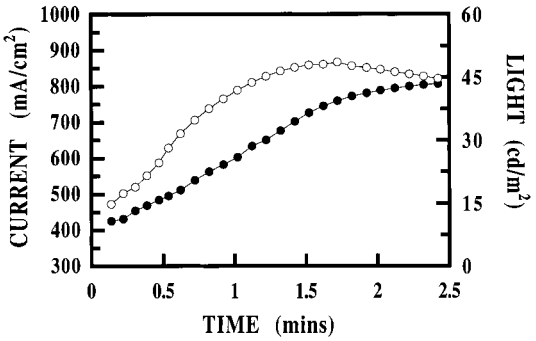

Figure 5. Light−time (open circles) and current−time (filled circles) plots for an ITO/Ru(phen)′$_3^{2+}$/Al device held at 6 V applied bias.

as expected for a device operating via an electrochemical mechanism. This is in contrast to polymer LED devices where rectification ratios greater than 10^4 are common.[45] However, the light−voltage plots are asymmetric about zero voltage. For the ITO/Ru(phen′)$_3^{2+}$/Al devices, light emission in reverse bias is negligible. With the ITO/(Ru(phen′)$_3^{2+}$ + PEO + $LiCF_3SO_3$)/Al devices, however, the situation is somewhat changed, where luminance levels of 1−3 cd/m^2 are observed in reverse bias. The absence of light is somewhat surprising considering that the current densities are sufficiently high for light emission. This would suggest that extensive quenching of the Ru(phen′)$_3^{2+*}$ occurs in the device during reverse bias operation or that competitive oxidation of the Al electrode is preventing the formation of the Ru(phen′)$_3^{3+}$ species that are needed to generate the light-emitting Ru(phen′)$_3^{2+*}$ excited state.

Murray et al. have shown that the electron hopping rates associated with the different redox reactions of the Ru(II) complex can be substantially different.[28,36] In addition, Bard et al. have reported that conductive metal electrodes act as more effective quenchers of Ru(phen′)$_3^{2+*}$ than semiconductor electrodes such as ITO.[21] Thus, differences in electron hopping rates could result in the light emission being spatially prone to the Al electrode under reverse bias conditions and hence a higher level of electrode quenching. This does not appear to be the case, however, as we have found that perfectly symmetric devices (in both light and current) can be realized by using more electrochemically inert electrodes such as platinum. It therefore appears that electrochemical oxidation of the Al electrode occurs during reverse bias operation and severely limits the amount of Ru(phen′)$_3^{3+}$ created.

It should be noted that recent experiments carried out in our laboratory have shown that when suitable interfaces are created between the Ru(II) complex and the Al electrode, completely symmetric devices also can be realized with ITO/Ru(II)/Al devices.[31] With suitable device engineering, it is therefore possible to obtain fully symmetric devices from these Ru(II) complexes, even in very thin films (<2000 Å).

Figure 5 shows the current−time and light−time plots obtained when an ITO/ Ru(phen′)$_3^{2+}$/Al device is maintained at 6 V. Devices were preconditioned as described in the Experimental Section. Under a constant voltage, the devices turned on essentially immediately; however, a further 1.5 to 2.5 min was required for the device to reach maximum luminance and current density. The dynamic response of these devices is determined by mass transport rates (counterion and Ru(phen′)$_3^{2+*}$) and electron hopping rates. The electron hopping rates themselves may, in turn, be tied to the rate of molecular motions, as close proximity of molecular orbitals is necessary

(45) Braun, D.; Heeger, A. J. *Appl. Phys. Lett.* **1991**, *58*, 1982.

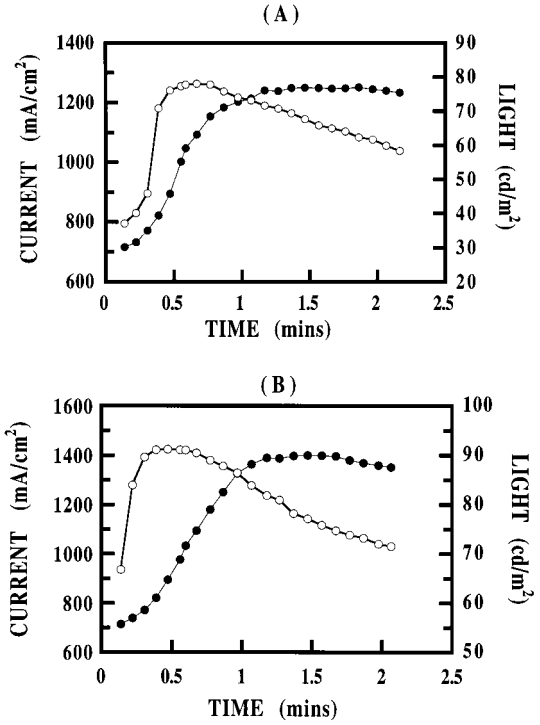

Figure 6. Light−time (open circles) and current−time (filled circles) plots for (a) an ITO/Ru(phen)′$_3^{2+}$ + PEO/Al device, and (b) an ITO/Ru(phen)′$_3^{2+}$ + PEO + $LiCF_3SO_3$/Al device held at 6 V applied bias.

for efficient electron transfer. Hence, the obvious "charging" effect associated with these devices is due to either limited counterion diffusion or limited ruthenium complex mobility or both.

Figure 6 shows the current−time and light−time curves for ITO/(Ru(phen′)$_3^{2+}$ + PEO)/Al and ITO/(Ru(phen′)$_3^{2+}$ + PEO + $LiCF_3SO_3$)/Al devices held at a constant voltage of 6 V. One would expect that when Ru(phen′)$_3^{2+}$ is dispersed in an ionically conductive PEO matrix with enhanced Ru(phen′)$_3^{2+}$ mobility the device response times would be faster (as well as higher current densities), and indeed this is found to be the case. At a constant voltage, the devices reach about 50% of their maximum luminance within a few seconds and reach maximum luminance in about 30 s. Although the dynamic response of the blend devices is improved, these are still relatively slow responding devices compared to those based on conjugated polymers.

Figure 6 also shows that at constant voltage, the light output of these devices starts to decay after about 45 s of operation. At 6 V, we have found that it takes about 1−2 h for the light output to decay to half its maximum value. At 4 V, devices can be operated for more than 100 h in either a nitrogen atmosphere or in air and still produce light detectable by the eye.[46] Over this time period, the light output typically drops from about 10 to 1 cd/m^2 and then appears to stabilize at the lower luminance level.

It is interesting to note that ITO/(Ru(phen′)$_3^{2+}$ + PEO)/Al and ITO/(Ru(phen′)$_3^{2+}$ + PEO + $LiCF_3SO_3$)/Al devices charge in roughly the same time. Both LiCl and $LiClO_4$ complexed PEO containing devices show similar results. These findings suggest that, at least within the time frame of these experiments, large scale counterion diffusion does not play the limiting role in determining charging times.

(46) Howie, D.; Rubner, M. F. Unpublished results, Massachusetts Institute of Technology.

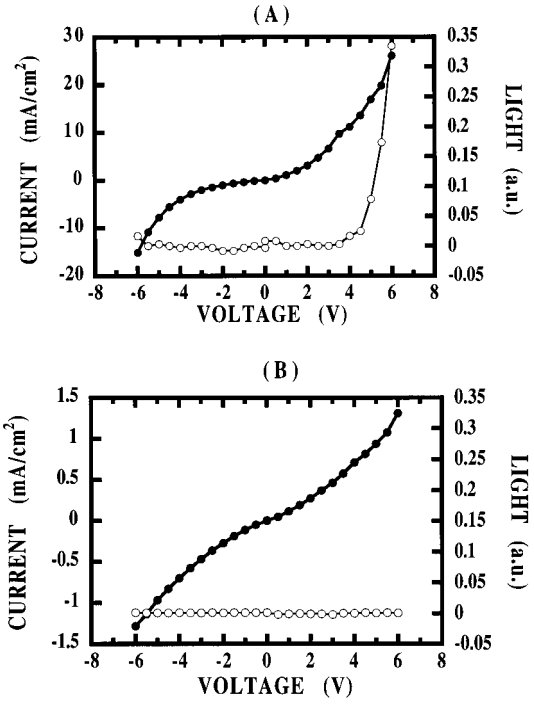

Figure 7. Light−voltage (open circles) and current−voltage (filled circles) plots for (a) an ITO/Ru(phen)′$_3^{2+}$ + PEO/Al device at 180 K preconditioned with 4 V at 295 K and (b) an ITO/Ru(phen)′$_3^{2+}$ + PEO/Al device at 200 K without voltage treatment at room temperature.

To explore this issue further, we examined the temperature dependence of these devices with and without a constant voltage preconditioning step. As noted in the Introduction, Maness et al. have recently described a procedure by which a serial concentration gradient of the $Ru^{III/II}$ and $Ru^{II/I}$ couples is established in a solid-state film of a Ru(II) complex through the application of a voltage under conditions of relatively high ionic mobility. This mixed valence state concentration gradient is then "frozen-in" by lowering the temperature of the sample to remove the ionic mobility while holding the voltage in place. The devices then exhibit diode-like behavior with fast response times, in contrast to the typical slow response times and symmetric current characteristics of a normal electrochemical device. If the voltage is not applied at room temperature, very little light or current is detected upon biasing at the lowered temperature. The authors show that the final "preconditioned" device operates by a process involving the transport of charge via a voltage-gradient-driven electron hopping. If the mixed state is already in place, the forward bias response time is no longer limited by the ionic mobility of the system and the reverse bias response is completely shut off when the device is driven opposite to the built-in gradient.

Following a protocol similar to the one described by Maness et al.,[28] we applied a 4 V positive bias to our thin film devices and held it while cooling to temperatures as low as 120 K (−153 °C), a temperature that is well below the glass transition of PEO (about −50 °C). Devices were then scanned to 6 V in positive or negative bias. Although, as expected for a thermally activated hopping process, the current levels were more than an order of magnitude lower than what was observed at room temperature, the basic device characteristics remained unchanged, i.e., current and light in the forward bias, and current of comparable magnitude in reverse bias but no light. These device characteristics are seen in Figure 7A (note that the absolute light output cannot be compared with the results presented in previous figures because the diode is farther from the sample in the low temperature setup and therefore captures less of the emitted light). Thus, in contrast to the behavior described by Maness, current is observed to flow readily upon applying a reverse bias at these very low temperatures, suggesting that the initially created concentration gradient is readily erased in these thin film devices within the time frame of the measurements. This is an interesting observation when one considers that ionic mobility at these very low temperatures should be highly quenched and yet it is still possible to readily obtain high current densities (in the 15−30 mA/cm^2 range at 180 K) in both the forward and reverse bias. At these low temperatures, an individual device can also be repeatedly cycled from forward to reverse bias more than 10 times, maintaining the same, nearly symmetric current values on each cycle and approximately the same light output in forward bias.

Devices were also tested at low temperature without the preliminary 4 V positive bias (see Figure 7B for a sample curve). In this case, the samples were not conditioned as described in the Experimental Section but were cooled as made, without ever experiencing a voltage bias until reaching the desired temperature. The current densities in these films were more than 2 orders of magnitude smaller than the room-temperature values, leading to light levels lower than the detection limit of the simple photodiode setup used. However, even though these measurements were made in some cases more than 100° below the T_g of the PEO matrix where ionic mobility is severely quenched, these unconditioned samples still maintained the basic characteristics of the room-temperature devices, i.e., comparable maximum current densities (about 1.5 mA/cm^2 at 200 K) in both the forward and reverse bias within the time resolution of the measurement. This result is in distinct contrast to the behavior observed by Maness et al. in which no light and current was observed if a voltage was not applied during cooling. It therefore appears that, although the establishment of a serial frozen concentration gradient in forward bias does appear to result in higher current densities, and therefore higher light output at lower temperatures, it is not the only means by which charge can be transported in these thin film devices.

To obtain more information about the origins of this interesting device response, we examined the temperature dependence of the charging effect observed in these films (vide Figure 6). This was accomplished by scanning the voltage of a device to 6 V, recording the "instantaneous" 6 V value, waiting 5 s, and recording the change that occurs in current over this time interval (voltage maintained at 6 V). At room temperature, we find that both current and light steadily increase when the device is turned on and held at this constant voltage. At lower temperatures, however, this charging hysteresis completely disappears and the device can be cycled reproducibly and repeatedly to constant current values in both the forward and reverse bias at greater than 20 V/s. This behavior is observed in both Ru(phen′)$_3^{2+}$ only and PEO-blend samples and in both constant-voltage preconditioned and neat samples. As illustrated in Figure 8, the onset of this charging hysteresis (observed by heating from low temperature) for a voltage preconditioned device containing the PEO−Ru(II) blend occurs around 200−220 K, close to the glass transition temperature of PEO. However, a similar onset temperature is observed in the Ru(phen′)$_3^{2+}$ only preconditioned devices (see Figure 8), indicating that this transition from a dynamically fast device with no observed charging behavior to distinct charging behavior is not related to an increase in ionic mobility brought about by the segmental motions activated in the PEO chains.

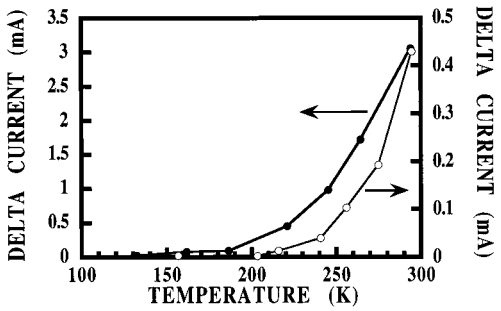

Figure 8. Current charging−temperature plots for preconditioned (filled circles) and untreated (open circles) ITO/Ru(phen′)$_3^{2+}$ + PEO/Al devices. Each sample was ramped to 6 V and held for 5 s. The difference between the current values before and after the voltage hold is plotted versus temperature.

All of these results suggest that there may be at least two modes of charge transport active in the thin films examined in this study: one that is relatively fast and remains active down to very low temperatures and one that is much slower and is only active down to about 220 K (−50 °C). At room temperature, the faster mode of charge transport gives rise to a nearly instantaneous light emission whereas the slower mode is responsible for the "charging effect" that further increases the current flow and hence light output at constant voltage. The charging behavior exhibited above 220 K is likely coupled to a relatively sluggish ionic transport process involving a microscopic rearrangement of the counterion population and the establishment of a more conductive mixed valence state concentration gradient. Recall, however, that in the voltage preconditioned devices, it is still possible to readily reverse the current flow by applying a reverse bias even at temperatures well below the point that the charging behavior is no longer observed. Thus, the higher current densities realized at low temperatures as a result of the preconditioning step are observed in both the forward and reverse bias, suggesting that it is possible to repeatedly erase the preestablished concentration gradient established in the forward bias at temperatures where ionic mobility should be highly quenched. This seems unlikely given what is known about the transport behavior of these materials and therefore indicates that an alternative mechanism may be needed to explain these results. More detailed studies are currently underway.

Clearly, much more work is needed to fully understand the mechanisms of charge transport operating in these thin film devices. We anticipate that many of the effects that we have observed are related directly to the very large electric fields that are typically applied across a device (about 5×10^5 V/cm), and the thin film nature of these devices (<2000 Å). Such conditions favor relatively facile ionic transport, at least at the nanoscale level, and thereby may allow for the establishment of a voltage gradient driven transport process that is readily reversed. It is also possible that, in addition to the expected redox conduction known to occur in these materials, there is also some level of charge transport that is facilitated via an electron hopping process not involving mixed redox states as is found in other small molecule and polymeric π-electron systems. The somewhat faster charging times observed in the blend systems (with and without any added salt) also seem to indicate that the ability of the Ru(II) complex to undergo local-scale molecular reorganizations may help to facilitate a more optimum electron hopping process.

It is clear that the behavior observed in thin film devices can be quite different from that observed in devices with larger electrode spacings.[28,29] This, in turn, suggests that different strategies may be needed to optimize the performance of thin film devices based on Ru(II) complexes. *Most importantly, this work clearly shows that elaborate charging schemes involving the use of elevated temperatures or solvent treatments that enhance ionic conductivity are simply not needed in these thin film devices. Devices of this type can be fabricated via conventional processing routes and conditioned to high light output and reproducible behavior with a few simple voltage scans.*

The thin film nature of these devices is clearly important. In the thickness range that we have currently explored (500 to 2000 Å), the turn-on voltage remains essentially constant (2.5−3.0 V) as do the device response times and external quantum efficiencies. However, at thicknesses greater than 2000 Å the turn-on voltage shifts to higher values. For example, a 2500 Å thick emitter layer device has an initial turn-on voltage of about 4 V. This effect can be explained in terms of an additional film resistance arising from limited ionic and electronic conductivities. Device response times are also slower and the external quantum efficiency begins to decrease. Clearly, as suggested above, the thin film nature of these devices is quite important in determining device behavior, which can change dramatically as one moves into a thicker film regime.

Finally, as expected for an electrochemically driven process, we have found that device turn-on voltage is not influenced by the type of cathode used to fabricate the devices. Devices fabricated with metals such as Al, Au, Pt, and Ag all exhibit turn-on voltages in the 2.5−3.0 V range. As noted earlier, devices fabricated with Pt electrodes exhibit completely symmetric device behavior in both light and current, as is expected for an electrochemically active device. In recent experiments in our laboratory, we have also found that patterned conducting polymer films can be utilized as the working anode of these devices with similar results.[47] These electrode materials are interesting from the point of view of flexible light-emitting devices.

Summary

We have demonstrated that thin-film light-emitting devices based on blends of Ru(phen′)$_3^{2+}$ + PEO + $LiCF_3SO_3$ can be conveniently fabricated. PEO functions both as a film processing aid, giving uniform and homogeneous devices, and as a polymer electrolyte for Ru(phen′)$_3^{2+}$ and counterions. Charge injection is via an electrochemical redox mechanism. The mechanism of light generation is likely similar to electrogenerated chemiluminescence. These devices offer a number of interesting and desirable features. Relatively low turn-on voltages of 2.5−3.0 V are observed. Turn-on and operating voltages are independent of film thickness up to 2000 Å. In addition, electrode materials such as Al, Ag, and Pt (and conceivably any stable conductive material) can be used, with reverse bias light output possible with electrochemically inert materials such as Pt.[48] At 6 V, luminance levels of 100 cd/m^2 can be obtained with an external quantum efficiency of about 0.02%. Devices reach about 50% of their maximum luminance within a few seconds, and reach maximum luminance in about 30 s. Preliminary investigations of the temperature-dependent behavior of these devices indicate that their thin-film nature

(47) Results to be submitted for publication.

(48) We thank a reviewer of this paper for pointing out the possibility of aluminum oxidation when operating in reverse bias.

may give rise to unusual charging dynamics and multiple charge transport mechanisms. This work also demonstrates that thin-film devices based on the Ru(II) complex can be fabricated by conventional processing means and activated to high brightness by simply scanning to suitable voltages. Finally, we note that recently other workers have also started to examine the Ru(II) complex as a solid-state light emitter.[49]

(49) Elliot, C. M.; Pichot, F.; Bloom, C. J.; Rider, L. S. *J. Am. Chem. Soc*. **1998**, *120*, 6781.

Acknowledgment. This work was supported in part by the MURI program of the Office of Naval Research, the Office of Naval Research, and the MRSEC program of the National Science Foundation under award number DMR-9400334. The authors are grateful to Professors Tripathy, Sandman, and Kumar of the University of Mass/Lowell for valuable discussions and Michael Durstock, Aiping Wu, and Erik Handy of MIT for assistance.

JA981057C